Optimal Sampling for Quantitative Magnetization Transfer

M. Cercignani[1], D. C. Alexander[2]

[1]NMR Research Unit, Intitute of Neurology,UCL, London, England, United Kingdom, [2]Centre for Medical Image Computing, Dept of Computer Science, UCL, London, England, United Kingdom

Introduction

We present a method based on the Cramer-Rao lower bound (CRLB) (1) to optimize sampling strategies for quantitative MRI techniques that estimate multiple parameters by fitting a model to the MR signal. We use the method for quantitative magnetization transfer (MT) imaging, which fits a model to images with MT pulses of variable amplitude ω and offset frequency Δ, and show significant error reduction in MT parameter maps.

Methods

Typically, quantitative MRI techniques fit a model S of a physical process with various unknown parameters $p_1 \ldots p_M$ to $N \geq M$ MRI measurements $A(\mathbf{x}_1) \ldots A(\mathbf{x}_N)$ acquired with different known settings $\mathbf{x}_1 \ldots \mathbf{x}_N$ in the pulse sequence. The precision and accuracy of the estimates of the parameters, p_i, $i=1 \ldots M$, depends on the sample positions $\mathbf{x}_n$, $n=1 \ldots N$. We aim to maximize the precision of the parameter estimates by finding the sample positions that minimize $\sum_{i=1}^{M} p_i^{-2} \sigma_i^2$, where σ_i^2 is the variance of p_i. The CRLB provides a lower bound on each σ_i^2, which is the i^{th} diagonal element of the inverse of the Fisher information matrix (1). The Fisher matrix has ij^{th} element $F_{ij} = \frac{1}{\sigma^2} \sum_{n=1}^{N} \frac{\partial S(p_1,\ldots,p_M;\mathbf{x}_n)}{\partial p_i} \frac{\partial S(p_1,\ldots,p_M;\mathbf{x}_n)}{\partial p_j}$, where σ is the standard deviation of background noise, which we assume is constant. Thus we optimize quantitative MRI by acquiring measurements at the $\mathbf{x}_n$ that minimize $V = \sum_{i=1}^{M} p_i^{-2} [F^{-1}]_{ii}$ for a typical set of p_i.

In qMT, the acquisition variables that define the sampling points are ω and Δ, so $\mathbf{x}_n = (\omega_n, \Delta_n)$. To illustrate the method, we use the MT model of Ramani et al (2), in which

$$A(\omega,\Delta) = gM_0 \frac{R_B\left[\frac{RM_0^A f}{(1-f)R_A}\right] + R_{RFB} + R_B + RM_0^A}{\left[\frac{RM_0^A f}{(1-f)R_A}\right](R_B + R_{RFB}) + \left(1 + \left[\frac{\omega}{2\pi\Delta f}\right]^2 \left[\frac{1}{R_A T_2^A}\right]\right)(R_{RFB} + R_B + RM_0^A)}.$$

We fit the model to measurements using a Levenberg-Marquardt algorithm, as in (4), to estimate six parameters: RM_0^A, $f/R_A(1\text{-}f)$, T_2^B, $1/R_A T_2^A$, R_B, and gM_0. Here, A and B label the liquid and the semisolid pools, respectively, and f is the bound proton fraction (2). In fact, the sum in V only includes the first four parameters, since we fix $R_B=1$ and gM_0 is of little interest. We use $N=10$. The global minimum of V is hard to find because V has many local minima. Thus, we use a minimization technique which combines simulated annealing with the downhill simplex method (3). Due to practical limitations on the combinations of ω and Δ, we constrain $\omega<955$ rad s^{-1} and $\Delta>0.15$ kHz.

Standard V=6.2		Optimized V=2.0	
ω	Δ	ω	Δ
222	0.4	40	42
222	1	130	100
222	3	262	0.15
222	7.5	400	1.38
222	20	400	1.48
885	0.4	400	1.48
885	1	955	0.97
885	3	955	0.98
885	7.5	955	0.98
885	20	955	11.6

Table 1. MT point schemes. ω is expressed in rad s^{-1}, Δ is expressed in kHz

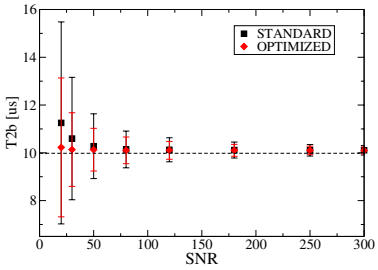

Fig 1. Plot of mean T_2^B from 10000 Monte Carlo simulations against SNR in the unweighted image. The error bars show the standard deviation. The dashed line shows the value of T_2^B used to create the simulation.

Experiments and Results

Table 1 compares the optimized sampling scheme returned by the minimization algorithm with a standard 10-point scheme (4). We use Monte Carlo simulations at various noise levels to measure the error in the parameters from the two acquisitions. Figure 1 confirms an improvement in both precision and accuracy for T_2^B at all SNR levels when using the optimized scheme; plots for the other parameters show similar trends. One subject was scanned twice on a 1.5 T system using a 3D MT-weighted fast SPGR sequence (TR/TE=28/5.1 ms, flip angle=5º, Gaussian MT pulses, duration=14.6 ms, 28 reconstructed slices). Three complete datasets were obtained using each scheme. In addition to the MT data, two 4-shot spin-echo EPIs (TR/TE=15000/13.6 ms, flip angles=60º and 120º, matrix 64x64), and 2 3D SPGRs (TR/TE1/TE2=16/4/8.54 ms, flip angle 25º) were collected for B_1 (5) and B_0-mapping (6), respectively. Figure 2 shows the MT parametric maps from each scheme using only the first repeat from each acquisition scheme. Maps from the optimized scheme show clear improvements in spatial homogeneity and grey-to-white-matter contrast. After image co-registration, Ramani's model was fitted to 1000 bootstrapped samples (accounting for B_1 and B_0 inhomogeneities) for each MT point scheme, providing 1000 estimates of RM_0^A, $f/R_A(1\text{-}f)$, T_2^B, $1/R_A T_2^A$, and gM_0. Table 2 compares the coefficient of variance (COV), defined as standard deviation divided by mean across the 1000 bootstrapped samples, of the MT parameters averaged over various regions of interest. The COV for the optimized scheme is consistently less than half that for the standard scheme, which confirms the significant improvement in parameter estimation observed in Fig. 2.

		GM1	GM2	WM1	WM2	WM3
RM_0^A	S	31	23	28	27	21
	O	11	8	11	13	9
$f/R_A(1\text{-}f)$	S	16	10	12	12	10
	O	6	4	5	7	5
T_2^B	S	18	10	8	10	9
	O	5	2	4	4	3
$1/(R_A T_2^A)$	S	15	10	10	11	10
	O	3	3	4	4	5

Table 2. Mean parameter COV [p.u.] across 1000 bootstrapped samples for the two schemes (S=standard, O=optimized). GM1=putamen; GM2=thalamus; WM1=genu of corpus callosum; WM2=anterior periventricular WM; WM3=posterior periventricular WM. Values are average of left and right for bilateral structures.

Discussion

We have shown significant improvements to MT parametric maps by the use of an optimal MT point sampling scheme. Simulations show increased accuracy in recovered parameters and experiments with bootstrapped brain data show increased precision. The new sampling scheme makes accurate and precise quantification of MT parameters feasible from data collected in clinically acceptable scan times. The method extends easily to other quantitative MRI techniques. Minor improvements may come from averaging V over a range of settings for the p_i during optimization, although preliminary experiments suggest that the optimal sampling we show is fairly insensitive to the exact p_i used in the optimization.

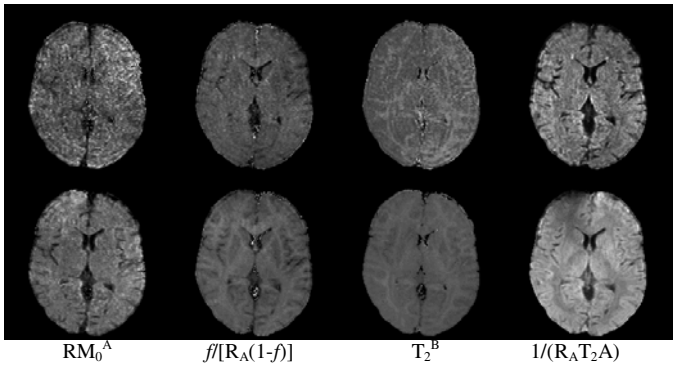

Fig 2. MT parametric maps obtained with the standard (top) and the optimized (bottom) sampling schemes.

References

1. Kay SM, Englewodd Cliffs, NJ, Prentice Hall 1993, p.27;
2. Ramani A, et al., Magn Reson Imaging 2002 ; 20 : 721-731;
3. Press WH et al.,Cambridge University press 1992; p 451;
4. Cercignani M. et al., NeuroImage 2005; 27: 436-41;
5. Stollberger R and Wach P, Magn Reson Med 1996; 35: 246-251;
6. Cusack and Papadakis, NeuroImage 2002; 16: 754-64.